Journal of Earthquake and Tsunami, Vol. 5, No. 2 (2011) 151–165

DOI: 10.1142/S1793431111001030

IDENTIFICATION OF DAMAGE IN REINFORCED CONCRETE COLUMNS UNDER PROGRESSIVE SEISMIC EXCITATION STAGES

ZHISHEN WU* and ADEKUNLE PHILIPS ADEWUYI
Department of Urban & Civil Engineering
Ibaraki University, 4-12-1 Nakanarusawa-cho
Hitachi 316-8511, Japan

SONGTAO XUE
Department of Architecture
School of Science & Engineering
Kinki University, Osaka, Japan

Accepted 17 July 2010

Prompt and accurate detection of realistic damage in constructed facilities is critical for effective condition assessment and structural health monitoring. This paper reports the experimental investigations of eccentric reinforced concrete columns mounted onto a shaking table and subject to progressively increasing seismic excitations. The investigation was aimed at studying the changes in the dynamic parameters in order to assess the structural conditions of the concrete columns after each post-seismic stage. The dynamic response of the structure was measured using accelerometers, traditional foil-strain gauges, and long-gauge fiber Bragg grating (FBG) sensors. The post-seismic conditions of the columns were evaluated via vibration-based damage identification methods. Results from this study demonstrate the applicability of specially packaged surface-mounted long-gauge FBG sensors for detecting the initiation and the progression of cracks due to reverse dynamic loads. The concept of modal macrostrain analysis was also introduced to identify and localize mild damage due to the applied seismic excitations of increasing intensities. The performance of the sensors for structural identification is also discussed.

Keywords: Progressive damage identification; dynamic analysis; modal macrostrain analysis; seismic excitations; FBG sensors.

1. Introduction

Civil infrastructure systems begin to deteriorate once they are built and subject to continuous or fatigue loading, occasional excessive loading, or extreme environmental conditions. In recent years, significant efforts have been devoted to developing non destructive techniques for damage identification in structures. Implementation of structural health monitoring (SHM) strategy on civil infrastructure systems is increasingly receiving attention due to factors such as construction defect, structural

*Corresponding author.

deterioration, material degradation and aging, harsh environmental conditions, changing of functionality, increase in loading demands, and the imminent risks of natural disasters. The contribution of these factors to the failure of civil infrastructure ranges from suboptimal performance to a complete breakdown. However, the conventional inspection-based maintenance concept can still not guarantee reliable structural integrity assessment and damage identification despite the huge cost.

Since the past few decades, research on vibration-based condition assessment and damage identification methodologies has been expanding very rapidly, as evidenced by comprehensive literature reviews covering practically all existing techniques and recent developments [Doebling *et al.*, 1998; Sohn *et al.*, 2003; Montalvao *et al.*, 2006]. The advent of vibration-based SHM techniques has advanced the need for prompt and reliable assessment of the performance and safety of civil structures, which hitherto receives attention only immediately after natural disaster or accidental damage. The traditional post-seismic visual inspection of structures, although provides knowledge about the vulnerability of structural systems and mechanisms of failure, is often unreliable for effective maintenance-based monitoring against major earthquakes [Bassam and Ansari, 2008]. The 1994 Northridge and 1995 Kobe earthquakes are major disasters that caused devastating damages to major civil infrastructure facilities whose financial loss was put at several billions of dollars. These catastrophic events confirmed the inability of the current state of knowledge in evaluating the level of excess ultimate capacity of structures, and the damage levels under various types of seismic activities [Bassam and Ansari, 2008; Lynch *et al.*, 2006; Zembaty *et al.*, 2006]. To achieve this goal, it is essential to investigate the response of bridges to the near-source ground motions, and to develop robust methodologies that would facilitate reliable prediction of bridge performance in real-time continuously or periodically after every occurrence of a medium-level earthquake.

Furthermore, the recent transformation of dynamic testing and analysis due to the major advances in the field of structural dynamics and mechanical vibration measurements has made it possible to evaluate the performance of constructed facilities on the basis of real-time data. It is desirable to measure the dynamic properties (resonant frequencies, mode shapes, and modal damping) of both the newly constructed and older existing bridges for a better understanding of their dynamic behavior under normal traffic loads as well as extreme natural disaster. Also, periodic monitoring of the dynamic properties is being studied for possible use as a method to assess degradation in the structural integrity of the bridge. The economic constraints make it practically impossible to monitor civil structures after each extreme event such as earthquake and typhoon. For a regular structure, special inspection after a small-to-medium seismic event is not necessary due to cost and the fact that such events pose little or no risk to the structural integrity. However, for more important structures such as high-speed railway bridges and long-span bridges, thorough inspection is inevitable for effective condition assessment and damage identification.

A considerable amount of research has been conducted in the area of vibration-based damage identification (VBDI) using modal parameters, such as changes in natural frequencies, mode shape, and its derivatives, modal flexibility and its curvature, modal stiffness, modal strain energy, frequency response functions (FRF), and their curvature and power spectral density in order to estimate the location and severity of the damage in structures [Farrar and James III, 1997; Sohn *et al.*, 2003; Carden and Fanning, 2004]. However, in spite of the in-depth research efforts in VBDI methodologies, several challenges still confront their practical application to large-scale civil structures. First, they cannot provide the accuracy and reliability required for complex system identifications of real life civil infrastructure due to the complicated behavior, the diversity of material properties, and incomplete, incoherent, and noise-contaminated measurements of structural response to excitations [Adewuyi *et al.*, 2009; Adewuyi and Wu, 2010a]. Second, modal frequencies are easy and accurate to measure by all manners of sensors, but they are neither spatially specific nor a reliable index for damage identification.

The type, quantity, and placement of sensors are very fundamental for accurate damage identification and successful implementation of SHM programs. Interestingly, the advent of fiber optic sensing strategies, especially fiber Bragg grating (FBG) sensors, has provided flexibility and practicality where the conventional sensors are either incapable or not feasible to make reliable measurements. In fact, FBG sensors are the most popular of all fiber optic sensing technology for civil infrastructure monitoring. When compared to traditional sensors used in experimental earthquake structural engineering such as accelerometers, velocimeters, potentiometers, displacement transducers, and resistive foil strain gauges, the FBG sensors are light, compact, flexible, immune to electro-magnetic interference, embeddable, and attachable to the host structure, and can be easily multiplexed in a large-scale distributed strain monitoring network. They also have unique ability to measure deformation over arbitrary gauge lengths with a resolution of less than one microstrain. Although strain is spatially specific and very sensitive to damage, the conventional foil strain gauges are not suitable for large-scale civil SHM not only because of the problem of stability, durability, and long-term reliability but also due to the inability to reflect the influence of damage effectively unless located at the damaged region [Adewuyi *et al.*, 2009; Adewuyi and Wu, 2010a, b].

The objective of this paper is to investigate damage in typical concrete columns under progressively increasing ground motions based on macrostrain measurements by long-gauge FBG sensors. Unlike several other investigations where damage was introduced through static or cyclic loading, which induces huge damages, dynamic characteristics of concrete columns are studied in this paper under progressive states of damage initiated only during normal operational conditions. This more practically and accurately simulate the situation often encountered in various earthquake zones. The existing modal curvature or modal strain algorithms are modified on the basis of the normalization of modal macrostrain measurements for effective damage localization in structures where (1) limited degrees of freedom are measurable,

(2) modal parameters from one or two fundamental modes can be identified, (3) damage severity is relatively small, and (4) measurement noise is inevitable.

2. Experimental Program

2.1. *Test set-up*

The progressive damage states of the structure is studied based on the structural dynamic response of the eccentrically loaded reinforced concrete (RC) columns of 150 mm square cross section and 1,200 mm high mounted on an MOOG world-wide support shaking table model G761-3502 as shown in Fig. 1. The experiments were conducted on a 0.9×0.9 m shaking table. Two eccentrically designed concrete columns, types A and B, reinforced with eight-6-mm-diameter-longitudinal bars with a mean yield stress, $f_y = 325$ MPa and Young's modulus of 165 GPa, and nineteen-4-mm-diameter stirrups spaced at 80 mm ($f_y = 180$ MPa, $E = 195$ GPa). The mean compressive strength, tensile strength, and Young's modulus of concrete are 41 MPa, 3.15 MPa, and 25.2 GPa, respectively.

A concentric axial load was introduced into the type A column using a steel bar pre strained to 2240 $\mu\varepsilon$ via a 10-mm-diameter bolt ($f_y = 407$ MPa, $E = 181$ GPa), while the type B column had no axial load. The two columns, cast monolithically to the 600 mm square base of 225 mm depth, were bolted onto the shaking table using eight-10-mm-diameter bolts. No additional load was added besides the uni directional base excitation by the shaking table. The mass of the bridge superstructure on the column is mimicked through an assumed inertial mass. The inertial mass is eccentrically loaded on the column to reflect practical conditions where the RC columns are designed to resist both the axial load and flexural moments. The

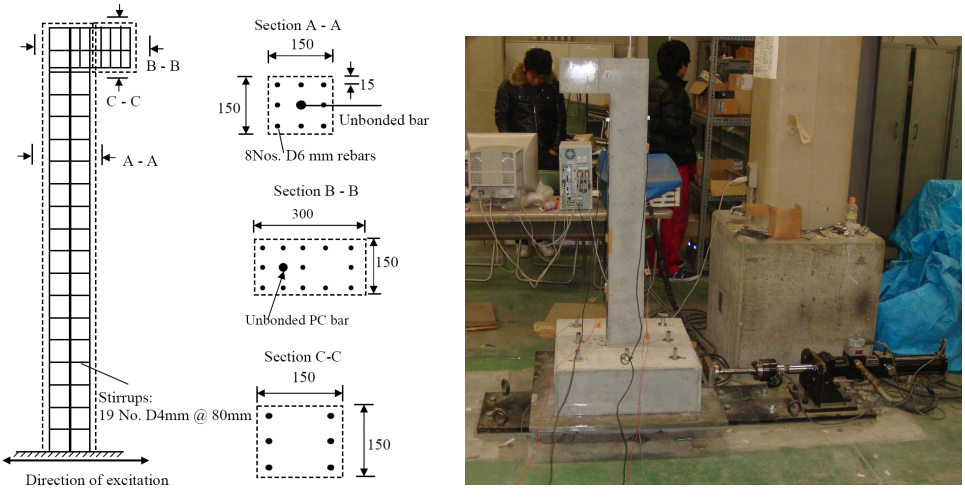

Fig. 1. Elevation and cross section of a typical column and the experimental set-up.

experiment was designed to monitor the structural health of eccentrically loaded RC columns for damage identification under varying seismic excitations to (1) study the changes in the modal parameters due to the development of cracks in the concrete column, and (2) detect and identify damage location in the concrete columns under progressively ground motions using the experimental data.

2.2. *Sensors and instrumentation*

The response of the columns to different seismic excitations was measured via accelerometers, electrical resistive dynamic strain gauges (DSG), and long-gauge FBG sensors. Each array of long-gauge sensors, designed and packaged in the authors' laboratory, consists of four serially multiplexed FBG sensors, three of which were of gauge length 100 mm and the last is of 200 mm. Basalt FRP tube were sprayed with wax until it penetrated into the tube. The basalt tubes were thereafter painted with resin and heated for 3 h. The multiplexed optic fibers were then encapsulated into the hardened basalt tubes, pre strained at two points to a predetermined strain in the range $1500 \sim 2000\,\mu\varepsilon$ and the end points of the fiber were glued onto a temporary support. The nodes between adjacent optic fibers of different wavelengths were reinforced with carbon FRP sheets of length 10 mm and the end points of the fiber was released after 12 h once the glue was cured. The sensor locations are shown schematically in Fig. 2. Two arrays of four FBG sensors were arranged on each face of the column as shown in Fig. 2 to capture the

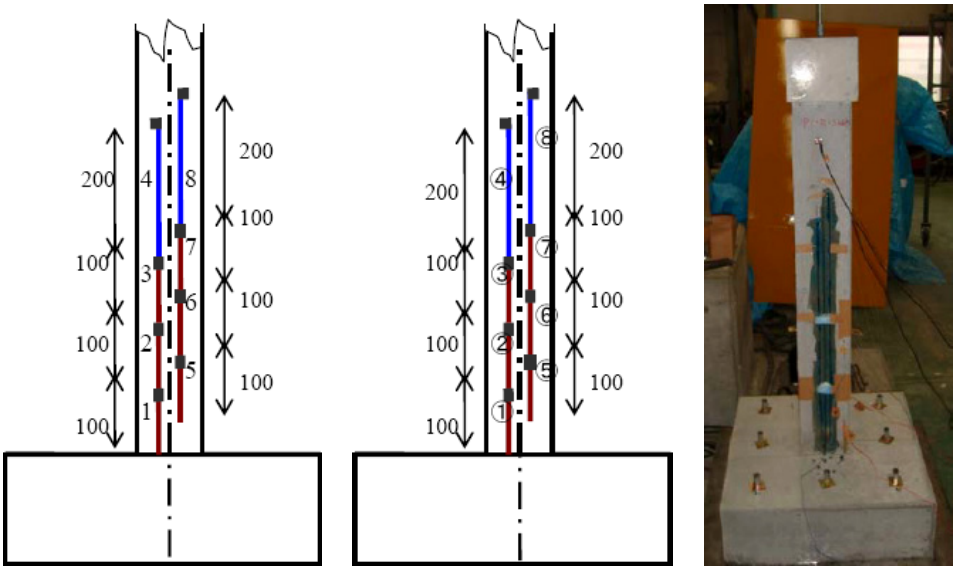

(a) (b) (c)

Fig. 2. Sensor arrangement: (a) sensor numbers — front view, (b) sensor numbers — rear view, and (c) photo of the sensor location.

occurrence of fine cracks, which might occur at the nodes between the adjacent FBG sensors.

The experimental program involved the application of ground motions to the column via the footing by the shaking table. The basic ground motions considered in the experiments included sine harmonic, sine sweep, and Kobe earthquake excitations. For each column, excitations were applied in three progressive stages of 15 successive excitations. (1) The columns were excited with small load amplitude at 15 successive times to measure the reference dynamic responses and identify the structure in an undamaged state S0. (2) The load amplitude was progressively increased to initiate change in the structural state after which 15 successive repetitions of smaller loads were applied to identify the dynamic properties at this stage S1. (3) The excitation level was further increased after which 15 successive repetitions of mild excitation were performed on the columns to assess the dynamic characteristics of the column as stage S2. It is worth stating that the excitation was so designed such that greater seismic loads were applied to type A compared to type B.

2.3. *Experimental results*

Modal parameters of the structures were identified from the response of the columns to ground excitations using the three sensor types collected at sampling rates of 500 Hz. The accelerometers and strain gauges were simply employed to assess the global vibration parameters of the structure in comparison to those obtained from FBG strain sensors. Typical acceleration and strain time histories are shown in Fig. 3. It is noteworthy that there was barely any difference between the strain measurements obtained from the staggered sensors shown in Fig. 2. For example, strain response obtained from sensors 1–4 is similar in pattern and magnitude to those obtained from 5–8. Thus, subsequent analyses were based on a single array of FBG sensors on the front and rear sides of the columns.

Figure 4 shows the power spectral densities (PSDs) extracted from the accelerometer and FBG strain sensor data. Only one mode was identified within the range $0 \sim 250$ Hz. The damping ratios were estimated based on the half-power bandwidth method. Stochastic subspace identification (SSI) method [Peeters and De Roeck, 1999] is a preferred modal identification technique especially in cases where the modes are not well separated. The natural frequency and the modal damping ratio corresponding to the first mode obtained from a typical acceleration and multiplexed FBG strain data for the RC column types A and B are shown in Table 1. As expected, it is obvious that the identified natural frequencies and damping ratios obtained from the three sensors have a good agreement. The variation in the frequency response of the column is in consonance with the level of damage due to the increasing levels of seismic loads. However, occurrence of damage was

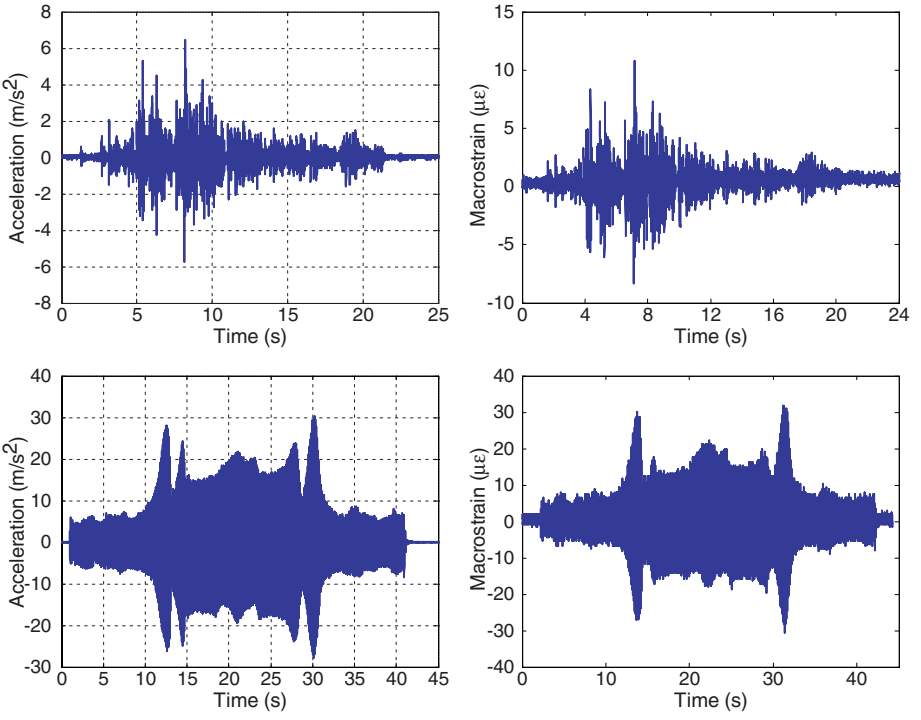

Fig. 3. Typical acceleration and the corresponding strain response to Kobe earthquake and sine sweep excitations.

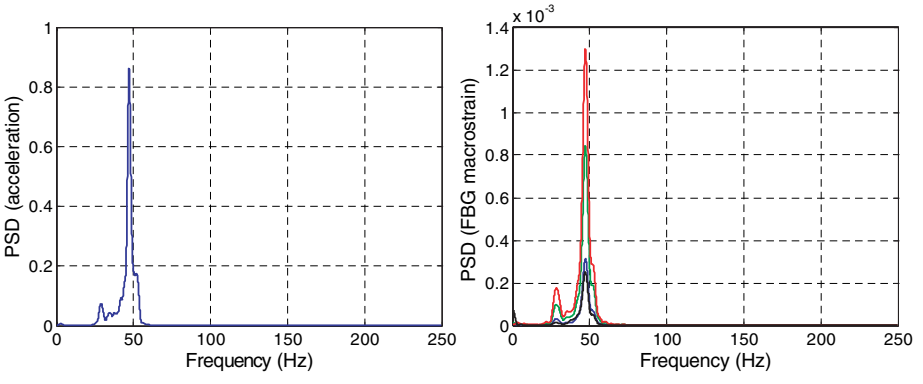

Fig. 4. PSD for typical acceleration and corresponding strain response measurements.

not discernible from the comparison of the frequency responses for the three stages of the columns. This shows that neither the frequency shift nor the modal damping ratio could independently give any clues about formation of plastic hinge in bridge columns.

Table 1. Natural frequencies and damping ratios identified from the first flexural mode of acceleration, strain gauge, and FBG's macrostrain data.

	Accelerometer		Strain gauge		FBG strain sensor	
Stage	Frequency (Hz)	Damping ratio (%)	Frequency (Hz)	Damping ratio (%)	Frequency (Hz)	Damping ratio (%)
RC column type A						
S0	47.24	3.31	47.26	3.28	47.25	3.35
S1	47.11	3.23	47.13	3.19	47.11	3.28
S2	47.01	3.10	46.99	2.94	47.02	3.09
RC column type B						
S0	47.12	2.90	47.14	3.01	47.13	2.88
S1	47.10	2.88	47.01	2.97	46.99	2.85
S2	47.01	2.91	46.90	2.95	47.92	2.80

3. Damage Identification Using Normalized Modal Macrostrain Index

A survey of technical literature reveals the availability of a number of methodologies for damage detection as well as damage localization by relating the change in modal parameters to mode shapes [Lieven and Ewins, 1988; Wolff and Richardson, 1989], mode shape curvatures [Pandey *et al.*, 1991], modal strain energy [Shi *et al.*, 2002; Stubbs *et al.*, 1995], and modal flexibility [Toksoy and Aktan, 1994]. Implementation of the above-mentioned techniques, which reflects the changes in mass and stiffness properties of the structure, requires that the modal parameters from the measured dynamic response are reliably identified. Various modal identification methodologies have been developed and modified for this purpose [Sohn *et al.*, 2003; Montalvão *et al.*, 2006]. Adewuyi *et al.* [2009] and Adewuyi and Wu [2010a, b] have highlighted the drawbacks of many of these methodologies using acceleration or displacement measurement techniques. Alternative condition and damage indices were also developed and validated using numerical simulation and experimental investigation. The extension of system identification methods to ambient vibration cases in civil engineering structures, in which input cannot be measured, is gradually receiving attention in technical literature.

There was no indication of damage in the type B column either via physical inspection or on the basis of variation of modal parameters. This was so because the column was subject to much lesser seismic excitations. On the other hand, fine cracks were observed in the type A column. The cracked column base with the surface adhered FBG sensors is shown in Fig. 5.

Modal identification of the RC column employed the frequency domain decomposition method (FDD) in which the singular value decomposition technique is used in conjunction with the PSD function of the structural response [Brincker *et al.*, 2000]. The FDD technique was employed in the computation of modal macrostrain vectors based on the fiber optic strain response history measured in four sensing locations at each face of the column. The mode shapes are normalized with respect

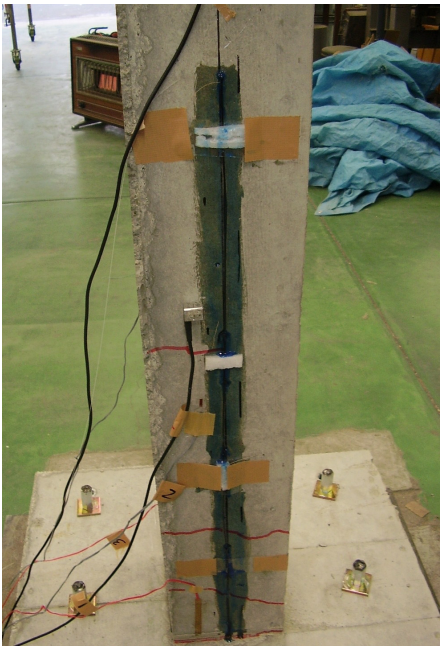

Fig. 5. Development of crack in the type A column after seismic events.

to the measured response at the FBG sensor furthest away from the maximum moment point at the base. The detailed procedure of normalization of modal macro strain (MMS) vectors can be obtained from Li and Wu [2008], and the change in normalized MMS algorithms can be found in Adewuyi and Wu [2010b] and Wu and Adewuyi [2009].

The location of the damage is assessed by the largest computed absolute changes in modal curvatures of the damaged and undamaged structure and is expressed in terms of the displacement and the MMS measurements, respectively, as

$$MC_i = \frac{1}{h_m} \sum_r \Delta\delta_{m_{ir}} = \frac{1}{h_m} \sum_r |\delta^d_{m_{ir}} - \delta_{m_{ir}}|, \tag{1}$$

where h_m is the distance from the surface of the structure where the sensor is installed to the inertia axis, δ_m is the modal macro strain obtained from the mth long-gauge, i and r are the indices for measurement location and mode, respectively, and the superscript (d) represents damaged structure.

The equation of motion of a structure with N degrees of freedom and viscous damping coefficients can be expressed as

$$[M]\{\ddot{x}(t)\} + [D]\{\dot{x}(t)\} + [K]\{x(t)\} = \{f(t)\}, \tag{2}$$

where $[M], [D]$, and $[K]$ are the $N \times N$ mass, damping, and stiffness matrices, respectively.

The modal characteristics of a linear freely vibrating undamped system are described by the following analytical eigenvalue equation

$$K\phi_r = \omega_r^2 M\phi_r \quad \text{for } r = 1, \ldots, n, \tag{3}$$

where ω_r and ϕ_r are the natural frequency and mode shape corresponding to the rth mode.

From experimental modal analysis (EMA), the strain FRF, $H_{jk}^{\varepsilon}(\omega)$, which relates the response at location j to a force at point k is given by [Maia and Silva, 1997]

$$H_{jk}^{\varepsilon}(\omega) = \sum_r \frac{{}_r\psi_j \cdot {}_r\phi_k}{M_r(\omega_r^2 - \omega^2 + i2\xi_r\omega_r\omega)}, \tag{4}$$

where ${}_r\psi_j$ represents the rth strain mode shape or MMS vector measured at location j, and ${}_r\phi_k$ is the displacement eigenvector of mode $r$corresponding to an excitation at the kth DOF, M_r is the modal mass, and ξ_r is the modal damping ratio.

Moreover, the magnitude of strain FRF at resonance for any mode r is given by

$$|H_{jk}^{\varepsilon}(\omega = \omega_r)| = \left(\frac{{}_r\phi_k}{2M_r\xi_r\omega_r^2}\right)_r \psi_j. \tag{5}$$

It is obvious from Eq. (5) that the quantity ${}_r\phi_k/2M_r\xi_r\omega_r^2$ is constant for any mode r. Many VBDI techniques are premised on the linearity of structural behavior in the pre- and post-damage states. The MMS vector Ψ_r comprising m components can be assembled as

$$\Psi_r = \{{}_r\psi_1 \quad {}_r\psi_2 \quad \cdots \quad {}_r\psi_j \quad \cdots \quad {}_r\psi_m\}^T. \tag{6}$$

A detailed theoretical modal analysis using displacement (or acceleration) and macro strain measurements is comparatively presented by Li and Wu [2008].

The vibration mode amplitudes obtained from an eigenproblem solution are arbitrary. In other words, any amplitude will satisfy an eigenvalue problem provided the resulting shapes are uniquely defined. Assume that dynamic tests are performed in succession, the ratio of the MMS at any measurement location to that of a reference sensor ${}_r\psi_{\text{ref}}$ of any gauge length remains constant unless there are changes in the dynamic properties of the structure. Hence, the normalized MMS vector $\bar{\delta}_{mr}$ is given by

$$\{\bar{\delta}_{1_r} \quad \bar{\delta}_{2_r} \quad \cdots \quad \bar{\delta}_{(m-1)_r} \quad \bar{\delta}_{m_r}\} = \left\{\frac{{}_r\psi_1}{{}_r\psi_{\text{ref}}} \quad \frac{{}_r\psi_2}{{}_r\psi_{\text{ref}}} \quad \cdots \quad \frac{{}_r\psi_{(m-1)}}{{}_r\psi_{\text{ref}}} \quad \frac{{}_r\psi_m}{{}_r\psi_{\text{ref}}}\right\}. \tag{7}$$

It is noteworthy that without loss of generality, normalized MMS vectors are non dimensional quantities, which have characteristic mode shapes analogous to the unnormalized MMS vector or the curvature mode shape. In addition, the normalization procedure is also applicable to displacement mode shapes, but previous findings have shown that it does not improve damage identification because as global quantities, they are not sensitive to damage.

The conventional modal curvature presented in Eq. (1) is modified in terms of the normalized MMS to enhance its sensitivity to mild damage as

$$NMMS_i = \sum_r \Delta(\bar{\delta}_{m_{ir}}) = \sum_r |(\bar{\delta}^d_{m_{ir}}) - (\bar{\delta}_{m_{ir}})|. \tag{8}$$

For any ground motion, the MMS vectors of each array of FBG sensors was identified based on the frequency domain decomposition technique earlier described. The target FBG sensors are designated as F1, F2, F3, and F4 according to their distance from the column base. F1 is the closest sensor to the base, while F4 (the 200-mm-gauge length) is the furthest from the column base. Since two arrays of FBG sensors are installed in parallel, one array was used as the target sensors, while one of the FBG sensors in the other array was selected as the reference. In this study, the FBG sensor of gauge length 200 mm was selected as the reference because it was the sensor with the least probability of damage. The plots of the MMS of the target sensors with respect to that of the reference sensor of the type A column for the seismic excitation states S0, S1, and S2 are presented in Fig. 6. The perfect best lines of fit were obtained in each case, which indicated that the structural behavior of the RC column was linear during these excitation states. As expected, the closer the target sensor to the base of the column where the moment is the highest the greater the slope or the normalized MMS is. Sensor F1 has the highest slope while F4 has the lowest slope.

For a clearer assessment of the performance and response of each sensor during different excitation states, the normalized MMS of each sensor is re plotted in Fig. 7.

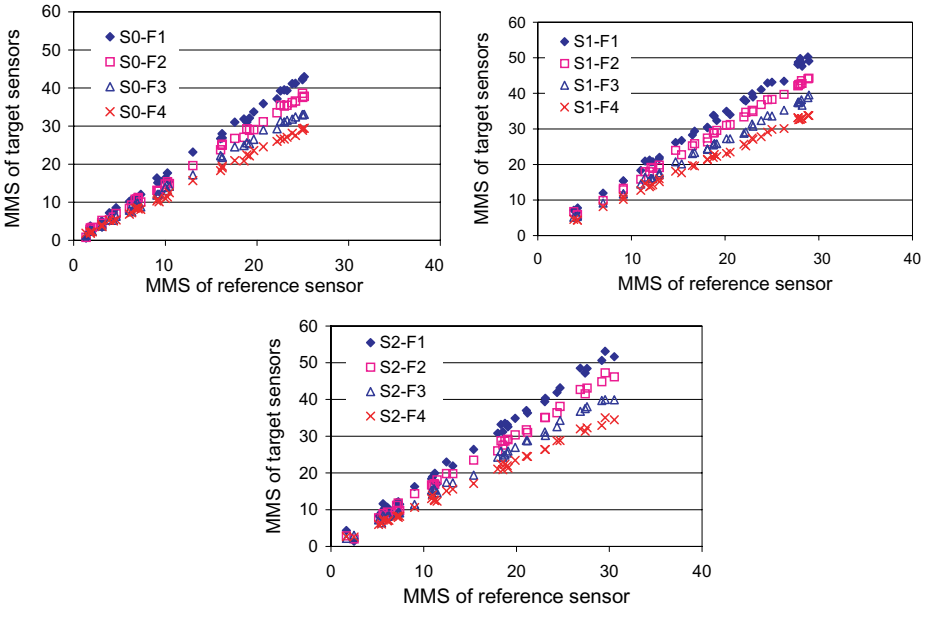

Fig. 6. Plots of MMS of target sensors relative to the reference for the three loading stages.

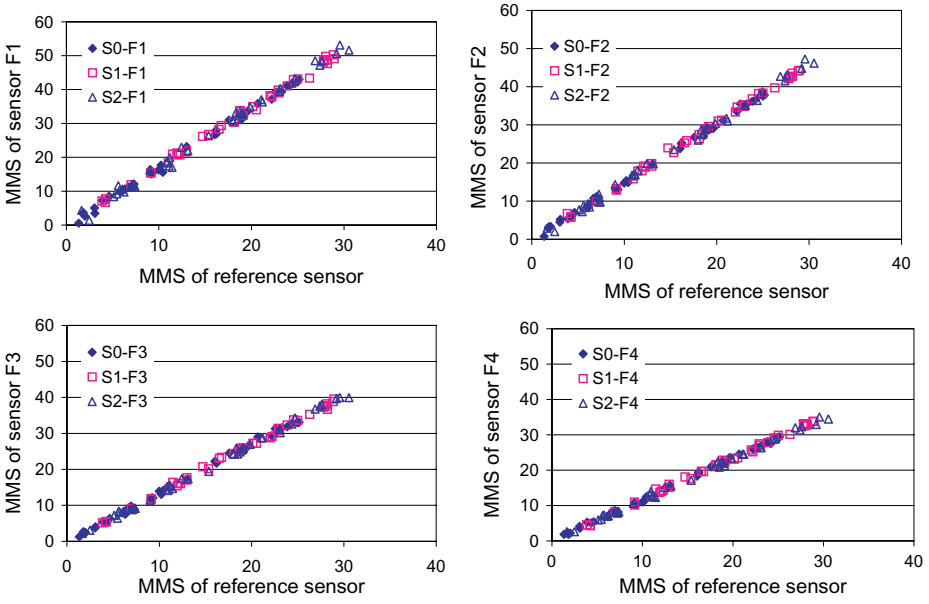

Fig. 7. Comparison of plots of normalized MMS for the three loading stages.

Each normalized MMS was produced on the same scale and the decreasing trend of the slope is very evident for the four target sensors. Moreover, although linearity of the normalized MMS is unmistakable for each target sensor, the slope change due to progressively increasing excitation states is not clearly identifiable. This can be attributed to the fact that damage occurrence in the column was very mild as indicated by the fine cracks on the column surfaces.

The numerical values of the slopes and the coefficients of correlation of the normalized MMS are presented in Table 2 for clarity. It is can be seen from the statistical features that the normalized MMS of the target and reference sensors are perfectly correlated. The remarkable changes in the normalized MMS as indicated by the slope of the lines of fits are boldly underlined in Table 2.

The plots of change in MMS and change in normalized MMS are presented in Fig. 8 for comparison. It is undoubtedly clear that the MMS and the normalized MMS are analogous as shown in Figs. 8(a) and 8(b). This implies that the

Table 2. Statistical features of slope or normalized MMS and the correlation coefficients.

	F1		F2		F3		F4	
Stage	Slope	R^2	Slope	R^2	Slope	R^2	Slope	R^2
S0	1.699	0.9972	1.522	0.9977	1.346	0.998	1.172	0.9982
S1	**1.733**	0.9966	1.523	0.9976	1.347	0.9975	1.171	0.9973
S2	**1.751**	0.9948	**1.537**	0.9965	1.348	0.9971	1.173	0.9965

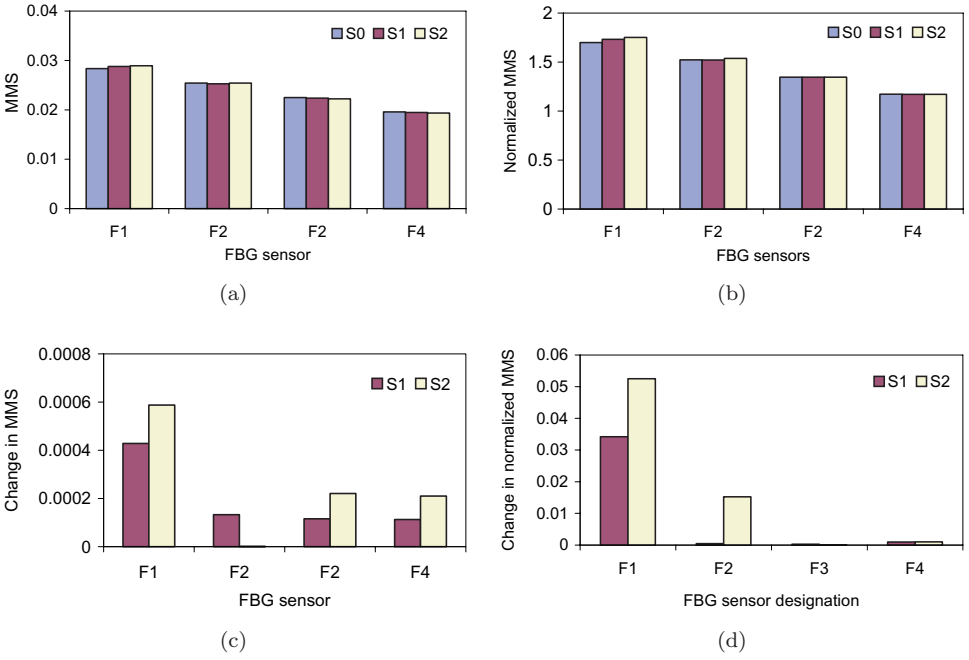

Fig. 8. Comparison between MMS and normalized MMS indices.

normalization does not change the eigenvector of the structure. However, it can be observed in Fig. 8(c) that it is difficult to correctly localize damage based on the difference between the MMS vectors in the damaged and undamaged states. In addition, the plot does not indicate the progressive damage trend in the column. The reason for this is that normal curvature mode or strain mode may not be sensitive to mild damage, but is a reliable index to identify and localize severe damage. On the other hand, the change in the normalized MMS shows the true trend of damage in the column as illustrated in Fig. 8(d).

It is conclusive that the proposed technique is very robust, efficient, and can effectively localize mild damage cases using few measurement data sources from one or two measurable modes.

4. Conclusions

The results of a shaking table experiment on structural damage identification and modal analysis of RC column under progressive damage has been presented. From the experimental investigation of a column, which depicts the behavior of a bridge column under normal operational condition, the dynamic characteristics of the columns were successfully identified using accelerometers, resistive foil strain gauges, and long-gauge FBG sensors. The natural frequencies and modal damping obtained from these sensors have a good agreement. Because the degree of damage

due to the progressively increasing seismic excitations is very mild, the natural frequency and modal damping ratio values could barely indicate occurrence of damage in the structures. Furthermore, the conventional modal curvature method, herein presented as MMS in terms of the strain mode shapes, could not reliably identify the location of damage in the column. However, damage trends and locations were successfully identified on the basis of the normalized MMS technique.

Finally, it can be inferred that although it is not economically viable to embark on special inspection of all regular civil structures after small-to-medium earthquakes owing to the cost and less risky effects, thorough inspection and prompt monitoring is very essential for effective condition and damage identification of more important structures such as high-speed railway bridge and long-span bridges.

References

Adewuyi, A. P. and Wu, Z. S. "Modal macro-strain flexibility methods for damage localization in flexural structures using long-gauge FBG sensors," *Struct. Control Health Monit.* http://dx.doi.org/10.1002/stc.377 (in press).

Adewuyi, A. P. and Wu, Z. S. "Vibration-based damage localization in flexural structures using normalized modal macrostrain techniques from limited measurements," *Comput.-Aided Civ. Infrastruct. Eng.* (in press).

Adewuyi, A. P., Wu, Z. S. and Serker, N. H. M. K. [2009] "Assessment of vibration-based damage identification methods using different measurement techniques," *Struct. Health Monit.* **8**(6), 443–461.

Bassam, S. A. and Ansari, F. [2008] "Post-seismic structural health monitoring of a column subjected to near source ground motions," *J. Intell. Mater. Syst. Struct.* **19**, 1163–1172.

Brincker, R., Zhang, L. and Andersen, P. [2000] "Modal identification from ambient responses using frequency domain decomposition," *Proc. 18th International Modal Analysis Conf.*, San Antonio, Texas, USA.

Carden, P. E. and Fanning P. [2004] "Vibration based condition monitoring: A review," *Struct. Health Monit.* **3**(4), 355–377.

Doebling, S. W., Farrar, C. R. and Prime, M. B. [1998] "A summary review of vibration-based damage identification methods," *Shock Vibr. Digest* **30**(2), 91–105.

Farrar, C. R. and James III, G. H. [1997] "System identifcation from ambient vibration measurements on a bridge," *J. Sound Vibr.* **205**(1), 1–18.

Li, S. Z. and Wu, Z. S. [2008] "A model-free method for damage locating and quantifying in a beam-like structure based on dynamic distributed strain measurements," *Comput.-Aided Civ. Infrastuct. Eng.* **23**(5), 404–413.

Lieven, N. A. J. and Ewins, D. J. [1988] "Spatial correlation of mode shapes, the co ordinate modal assurance criterion (COMAC)," *Proc. 6th International Modal Analysis Conf.* **1**, 690–695.

Lynch, J. P., Wang, Y., Lu, K. C., Hou, T. C. and Loh, C. H. [2006] "Post-seismic damage assessment of steel structures instrumented with self-interrogating wireless sensors," *Proc. 8th National Conf. on Earthquake Engineering* (*8NCEE*), San Francisco, California, USA [on CD ROM].

Maia, N. M. M. and Silva, J. M. M (eds.) [1997] *Theoretical and Experimental Modal Analysis* (Research Studies Press, Baldock).

Montalvão, D., Maia, N. M. M. and Ribeiro, A. M. R. [2006] "A review on vibration-based structural health monitoring with special emphasis on composite materials," *Shock Vibr. Digest* **38**(4), 295–324.

Pandey, A. K., Biswas, M. and Samman, M. M. [1991] "Damage detection from changes in curvature mode shapes," *J. Sound Vibr.* **145**(2), 321–332.

Peeters, B. and De Roeck, G. [1999] "Reference-based stochastic subspace identification for output-only modal analysis," *Mech. Syst. Signal Process.* **13**(6), 855–878.

Shi, Z. Y., Law, S. S. and Zhang, L. M. [2002] "Improved damage quantification from elemental modal strain energy change," *J. Eng. Mech.* **128**(5), 521–529.

Sohn, H., Farrar, C. R., Hemez, F. M., Shunk, D. D., Stinemates, D. W. and Nadler, B. R. [2003] "A review of structural health monitoring literature: 1996–2001," Los Alamos National Laboratory Report, LA-13976-MS.

Stubbs, N., Kim, J. T. and Farrar, C. R. [1995] "Field investigation of a nondestructive damage localization and severity estimation algorithm," *Proc. 13th International Modal Analysis Conf.* **1**, 210–218.

Toksoy, T. and Aktan, A. E. [1994] "Bridge-condition assessment by modal flexibility," *Exp. Mech.* **34**(3), 271–278.

Wolff, T. and Richardson M. [1989] "Fault detection in structures from changes in their modal parameters," *Proc. 7th International Modal Analysis Conf.* **1**, 87–94.

Wu, Z. S. and Adewuyi, A. P. [2009] "Vibration-based structural health monitoring technique using statistical features for data stability assessment and damage localization," *Proc. SPIE*, Vol. 7292, pp. 729233–729233-11.

Zembaty, Z., Kowalski, M. and Pospisil, S. [2006] "Dynamic identification of a reinforced concrete frame in progressive states of damage," *Eng. Struct.* **28**, 668–681.